Ship's Turbulent Propeller Wake: Combined Swirling and Linear Momentum Wake

James K.E. Tunaley

***Abstract*---The propeller wake from a ship may be important for an understanding of ship wakes in radar images. Interpretation of wake imagery promises to be useful in wide area maritime surveillance using satellites. A rotating propeller creates a wake, which can be visualized as a rotating horizontal column of water with both linear and angular momentum. This slowly broadens astern due to eddy diffusion as water surrounding the column becomes entrained within the wake. Purely linear momentum and purely angular momentum wakes are quite well understood both in theory and in practice. The purpose of this paper is to examine the combination of these wakes as occurs for a ship's propeller. The result is illustrated by applying it to the Queen of Alberni ferry.**

***Index Terms*---Ship wake, turbulent wake, swirling wake.**

I. Introduction

PROPELLER WAKE flows may be responsible for some of the characteristics of ship wakes in radar images taken by satellites [1]. This is because surface flows affect the radar backscattering coefficient. Though there are several kinds of ship wake, the most common is the "turbulent" wake [2]. A turbulent ship wake often appears as a dark line behind the ship in a radar image; these lines can be flanked by one or more thin bright arms. Therefore, to understand the potential of the turbulent wake to contribute towards maritime security, it is important to be able to predict the surface flows.

The turbulent wake has been studied in the laboratory [3,4,5]. In its simplest form an obstacle is placed in a fluid flow and the properties of the wake downstream are measured. These typically include the mean fluid velocity and the covariances of the velocity components as a function of position. The functionality of the variables in the distance downstream is often close to a power law.

The theory of turbulence is still a research topic because the full equations are non-linear and the behavior of a parcel of fluid depends on non-local conditions within the turbulent flow. To obtain solutions to simple problems, dimensional analysis is often used [6]. Another approach is to assume self-similarity [7]. This implies that various parameters of interest are similar throughout the wake apart from scale factors. Self-similarity is consistent with some experiments and tends to lead to power law behavior [5]. A problem with these methods is that they do not provide much physical insight.

Prandtl's mixing length theory [8] is perhaps the most satisfactory for the present purposes though it has its own fundamental problems. The theory is based on the concept of eddy diffusion, in which a parcel of fluid moves randomly as in molecular diffusion. However, the diffusion coefficient depends on the global parameters of the current solution; for wakes it depends on the width of the wake at that time and the difference between the mean flow in the wake and that outside it.

The utility of Prandtl's theory has been confirmed in the laboratory for the far wake of two-dimensional obstacles and for cases of axisymmetric obstacles. The wake characteristics are found to depend on the Reynolds number, R, which is dimensionless and represents the ratio of inertial forces to viscous forces. It is given by:

$$R = \frac{UL}{\nu} \tag{1}$$

where U is the flow velocity, L is a characteristic length, such as the length or diameter of the obstacle and ν is the kinematic viscosity, which is about 10^{-6} $m^2.s^{-1}$ for water at normal temperatures. For ships, R ranges between 10^7 and 10^9. However, in the laboratory, the Reynolds number tends to be very much smaller so that care must be exercised in interpreting results.

II. Wake Characteristics

Turbulent flows are described by the Navier-Stokes equation, which is non-linear. Water is approximately a Newtonian fluid so that dissipation can be described by a simple viscosity term. The non-linear behavior is associated with inertial terms and this is responsible for the chaotic type of fluid motions in a turbulent wake. Viscosity attenuates these chaotic motions. At high Reynolds numbers, the inertial terms completely dominate the wake and energy dissipation only occurs at small scales or far down the wake where the mean velocity is small and $R \sim 1$. In turbulence theory, the characteristic length used in R could be the size of an eddy or the wake width.

Even at high Reynolds numbers, a memory of the initial conditions in the flow persists far downstream. Therefore the way in which the wake is created is important. There are a limited number of simple cases for which there are solutions. The two-dimensional obstacles are not relevant here and so the focus is on the axisymmetric cases. These can be divided into the linear-momentum wake, the angular-momentum wake, the zero-linear-momentum wake and the zero-angular-momentum wake.

A zero-linear-momentum wake can be created when a submerged axisymmetric obstacle is driven at constant velocity by an axial jet. The zero-linear-momentum wake is very sensitive to the balance of linear-momentum [9]. It is not usually pertinent to the radar wakes of surface ships at service speeds because wave-making resistance typically ensures that the magnitude of the momentum production of the jet or propeller greatly exceeds that of the obstacle itself.

A zero-angular-momentum wake is created by two concentric paddles rotating in opposite directions. (The theory can be based

Published April 2010 and with minor corrections December 31st 2010.
J.K.E. Tunaley is with London Research and Development Corporation. Web: www.london-research-and-development.com.

on an extension of the method adopted by Birkhoff and Zarantonello [7] for the zero-momentum wake but will not be addressed here.) This is not appropriate to most surface ships because the torque from a single screw is typically balanced by a gravitational torque. Counter rotating twin screws generate zero angular momentum but the source is not axisymmetric. A contra-rotating screw is a case for which the zero-angular momentum wake would be relevant; it would typically be combined with a linear-momentum wake.

Table 1 summarizes the theoretical results for the far wakes of four canonical cases. Exponents p and q determine how the mean fluid velocities, u, fall off with axial distance, z, and radial distance, r:

$$u = Cz^q f(r / z^p) \tag{2}$$

where C is a constant and f is some function. The exponent, s, determines how the Reynolds number, defined using the wake width and u at r = 0, falls off with axial distance, z:

$$R = C_R z^s \tag{3}$$

TABLE 1
WAKE EXPONENTS

Wake Type	**p**	**q**	**s**
Linear-momentum	1/3	-2/3	-1/3
Angular-momentum	1/4	-3/4	-1/2
Zero-linear-momentum	1/5	-4/5	-3/5
Zero-angular-momentum	1/6	-5/6	-2/3

III. COMBINED WAKE

Prandtl's mixing length theory is based on the assumption that the rate of expansion of the wake diameter, b, is proportional to the maximum mean flow speed, u_0, relative to the surrounding fluid [8]:

$$\frac{db}{dt} = \beta u_0 \tag{4}$$

where β is a constant that is determined by experiment. For an axisymmetric linear momentum wake, the linear momentum of a fixed length of the wake is conserved. This is because, as new fluid is entrained, no external forces are involved. The thrust provided by the propeller can be related to the rate of production of linear momentum (Newton's second law), P′. In the far wake, observations indicate that the mean velocity profile is close to Gaussian [5] and the flow relative to the surrounding fluid is small. Therefore we have:

$$\begin{aligned} P' &= 2\pi\rho U \int_0^\infty u_0 r \exp(-4r^2 / b^2) dr \\ &= \pi\rho U u_0 b^2 / 4 \end{aligned} \tag{5}$$

The argument of the Gaussian factor has been chosen so that the rate of linear momentum production is similar to that of a cylindrical column of fluid of length U and diameter b moving at speed u_0.

In the ship frame of reference, the wake mean parameters are stationary so that equation (4) becomes:

$$U\frac{db}{dz} = \beta \frac{4P'}{\pi\rho U b^2} \tag{6}$$

This can be integrated to yield:

$$b = \left(\frac{12\beta P' z}{\pi\rho U^2}\right)^{1/3} \tag{7}$$

In the purely swirling wake, the flow just aft of the propeller disk is in the form of a horizontal rotating cylinder of fluid. To a first approximation the initial angular velocity within this cylinder is constant. As fluid is entrained by eddy diffusion and the wake broadens, angular momentum at the edge of the cylinder is transferred to the entrained fluid; the angular velocity of the new fluid will be increased, while that in the original cylinder will be decreased. Because the process resembles normal diffusion (of vorticity), it is reasonable to suppose that the angular velocity, ω, will eventually adopt a Gaussian profile in the radial direction.

The rate of production of angular momentum in the fluid, J′, in the far wake is given by:

$$\begin{aligned} J' &= 2\pi\rho U \int_0^\infty \omega_0 r^3 \exp(-4r^2 / b^2) dr \\ &= \frac{\pi\rho U \omega_0 b^4}{16} \end{aligned} \tag{8}$$

where ω_0 is the angular velocity along the axis of the wake. The profile in the angular velocity is similar to that of the linear momentum wake, as will be explained shortly. The maximum azimuthal velocity, $v_0 = \omega r$, occurs at r = b/4 and is given by:

$$v_0 = \frac{\omega_0 b}{\sqrt{8e}} \tag{9}$$

Expressing v_0 in terms of J′ yields:

$$v_0 = \frac{8J'}{\sqrt{2e}\,\pi\rho U b^3} \tag{10}$$

In the same way as for equation (5) and noting that angular momentum is constant, integration yields:

$$b = \left(\frac{32\beta J' z}{\sqrt{2e}\,\pi\rho U^2}\right)^{1/4} \tag{11}$$

and, once b has been determined, the azimuthal velocity at distance r can be found from equation (8):

$$v = \frac{16J' r}{\pi\rho U b^4} \exp(-4r^2 / b^2) \tag{12}$$

Evolution of a wake with both linear and angular momentum involves eddy creation and diffusion from both types of velocity shear. Eddies are likely to be created independently by each mechanism but an eddy transferring linear momentum to another radius will also transfer angular momentum. In contrast to the existence of independent wakes superimposed, which would be described by two wake radii, the wake will have one radius at any particular time; this explains why the same profiles are used in equations (5) and (8).

Because the process resembles ordinary diffusion, which is a stochastic process in which variances of independent sources of diffusion add, we modify the right hand side of equation (4) so that it becomes:

$$\frac{db}{dt} = \beta\sqrt{u_0^2 + v_0^2} \tag{13}$$

Once again the wake is stationary in the reference frame of the ship and we have:

$$\frac{\pi\rho U^2 b^3}{4\beta P'}\frac{db}{dz} = \sqrt{b^2 + a^2} \tag{14}$$

where the parameter a, which has the dimensions of length, is given by:

$$a = \frac{\sqrt{2}\,J'}{\sqrt{e}\,P'} \tag{15}$$

Therefore the following integral is required; this can be evaluated by a simple substitution and integration by parts:

$$\int_0 \frac{b^3 db}{\sqrt{b^2 + a^2}} = \frac{\sqrt{b^2 + a^2}}{3}\left(b^2 - 2a^2\right) + \frac{2a^3}{3} \tag{16}$$

It can be verified that, when a << b, the right hand side is equal to $b^3/4$ and, when a >> b, it tends to $b^4/(4a)$.

The relation between the wake width, b, and the distance astern, z, for the combined wake is:

$$\frac{\sqrt{b^2 + a^2}}{3}\left(b^2 - 2a^2\right) + \frac{2a^3}{3} = \frac{4\beta P'(z - z_0)}{\pi\rho U^2} \tag{17}$$

where z_0 is a constant of integration.

To estimate the parameters in the above equations for a ship at a given speed, it is necessary to estimate the viscous drag force on the hull, the form drag, the wave making resistance and the wind forces. The viscous hull drag can be estimated reasonably accurately and there exist factors to account for the other forces except wave making. The last of these increases rapidly with speed and starts to dominate the other forces at the ship's service speed. Therefore, as a first approximation it is reasonable to equate the wave making resistance to the viscous drag. From Newton's second law, at constant velocity the propeller thrust must be equal to the net drag force.

The rate of production of linear momentum in the propeller wake must equal the propeller thrust from Newton's second and third laws. Therefore an estimate of the drag forces yields a rate of production of linear momentum in the propeller wake. It is often assumed that energy is also conserved, at least approximately. This is reconciled to the momentum considerations through the conservation of mass and by noting that the cross section of the stream tube passing through the circumference of the propeller disk is not constant but decreases as the fluid is accelerated [10].

The rates of momentum and angular momentum production can be estimated for a given ship using theory based on the actuator disk model together with experimental observations on stock propellers in open water. The work done by the torque at the propeller is equal to the work done by the thrust in opposing the drag along with the kinetic energy of the water gained during its acceleration and its rotation as it passes through the propeller. The translational and angular velocities in the propeller race some distance aft of the propeller can be estimated in terms of the propeller slip ratio, σ, and the propeller efficiency, η. Effectively Comstock [10] shows that:

$$a' = 1 - \eta(1 + \sigma/2) \tag{18}$$

where a′ is the fraction of the power at the propeller converted into rotation of the fluid. A typical curve of efficiency of against slip ratio is provided in [10] for a four bladed propeller with a pitch ratio of one. For example, if η= 0.6 and σ = 0.4, as would be quite common for a large ship moving at its service speed, a′ ~ 0.3.

To illustrate this, the wake of the ferry, the Queen of Alberni, will be estimated. This is a double ended ferry operated by BC Ferries; it is driven by a single screw at the stern while the screw at the bow is feathered. Likely parameters are shown in Table 1 and were obtained from various sites on the Internet. The propellers of this ship are quite close to the surface.

Table 2 shows some derived quantities that affect the wake. The value of β is taken from [8], though the value was obtained for a two-dimensional obstacle. The drag factor was estimated from empirical data in [10].

Fig. 1 shows the wake diameter from the theory of combined linear and angular momentum wakes as well as from the individual wake theories. The effect of the free surface is neglected. As expected the angular momentum affects the combined wake close to the propeller but, far astern, the wake is controlled by linear momentum. The wake width exponent lies between those of the individual wakes at about 0.3 and the effect extends back for over 1 km. No attempt has been made to determine z_0, which has been set at zero.

The maximum surface flow velocities are shown in Fig. 2. These occur directly above the propeller axis. Close to the ship the swirl velocity dominates the axial flow but further astern the flow is primarily axial. The free surface has been taken into account by doubling the surface velocities, which would be expected if the surface were represented by an image of the wake above it. In the combined wake, the wake diameter expands more rapidly than either of the individual wakes separately. This reduces the surface flow velocities; the swirling velocity component decreases much more rapidly with distance than occurs in a pure angular momentum wake.

TABLE 1
QUEEN OF ALBERNI PARAMETERS

Parameter	**Value**
Length (m)	139
Maximum Beam (m)	27.1
Mean Draft (m)	5.5
Maximum Draft (Prop. Tip, m)	5.72
Block Coefficient (estimated)	0.6
Number of Propellers	1
Number of Blades	4
Mean Propeller Shaft Depth (m)	3.0
Propeller Diameter (m)	5.0
Propeller Type	CPP
Service Speed (knots)	19
Propeller Speed @ 19 knots (rpm)	~170
Propeller Efficiency (estimated)	0.6
Slip Ratio (estimated)	0.4
Maximum Power (MW)	8.83

The effect of the propeller depth is in shown in Fig. 3. The data for the Queen of Alberni has been modified with the screw axis depth set at 6 m rather than 3 m. The characteristics of these curves are typical of cargo ships; the velocities first increase with distance astern and then decrease. They are also generally reduced as the screw depth is increased.

TABLE 2
DERIVED AND OTHER PARAMETERS

Parameter	**Value**
Beta	0.2
Form and Appendages Drag Factor	1.3
Viscous Drag (N)	$2.4x10^5$
Linear Momentum Rate, P′ (kg.m.s^{-2})	$4.8x10^5$
Initial Wake Angular Velocity (rad.s^{-1})	2.85
Angular Momentum Rate, J′(kg.m^2.s^{-2})	$1.7x10^6$
Shaft Power (MW)	7.9

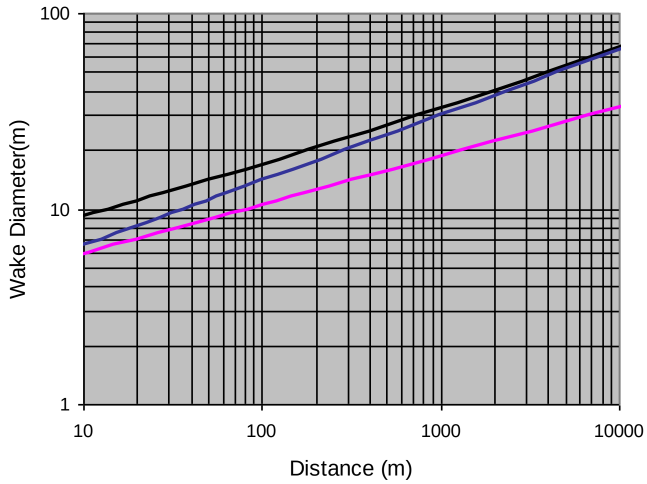

Fig. 1. Estimated wake diameters as a function of distance astern for combined wake (—), angular momentum wake (—) and linear momentum wake (—) for the Queen of Alberni.

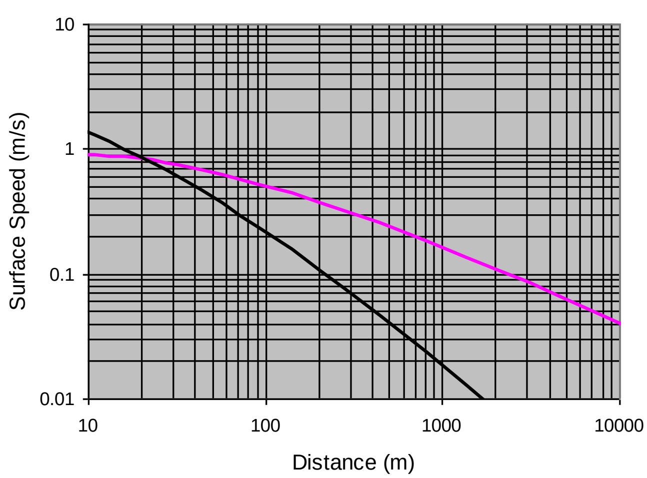

Fig.2. Maximum surface velocities in the propeller wake of the Queen of Alberni for swirl (—) and axial (—) components.

IV CONCLUSIONS

A theory has been developed for the combined linear momentum and angular momentum wake. This is based on assumptions that have been successful in predicting wake characteristics plus the assumption that the wake angular velocity profile is Gaussian. Even if for some reason these assumptions are not acceptable, the method provides a convenient means of interpolating between the two types of wake. Moreover, it can be extended to other wake combinations.

The approach has been illustrated by applying it to a ship. The combined wake diameter expands with an exponent lying between the two individual exponents and the surface velocity of the swirling component of surface velocity tends to exceed that of the axial component close to the ship. Because radar scattering depends partly on surface flows, this suggests that turbulent wake visibility in radar imagery often depends mainly on the swirling component because the swirl flows near the ship are usually larger.

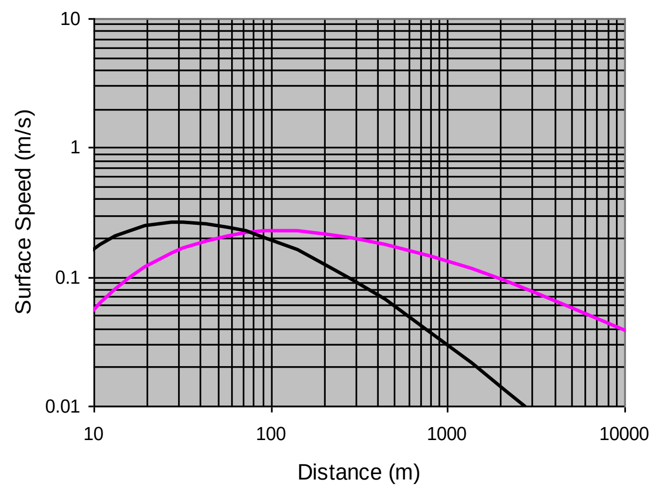

Fig. 3. Maximum surface velocities in the propeller wake of a hypothetical cargo ship with deep screws for swirl (—) and axial (—) components.

REFERENCES

[1] D.M. Roy, and J.K.E. Tunaley, Visibility of Turbulent Ship Wakes in Dual-Polarized RADARSAT-2 Imagery, Royal Military College and London Research and Development Corporation Report, January, 2010.
[2] J.D. Lyden, D.R. Lyzenga, R.A. Shuchman and C.V. Swanson, SAR Detection of Ship-Generated Turbulent and Vortex Wakes, Environmental Research Institute of Michigan Report RR-86-112, 1986.
[3] E. Naudascher, Flow in the Wake of Self-Propelled Bodies and Related Sources of Turbulence. J. Fluid Mech., vol. 22(4), pp 635-656, 1965.
[4] H. Higuchi and T. Kubota, Axisymmetric Wakes behind a Slender Body Including Zero-Momentum Configurations, Physics of Fluids A, vol. 2(9), pp 1615-1623, 1990.
[5] A.I. Serviente and V.C. Patel, Experiments in the Turbulent Near Wake of an Axisymmetric Body, AIAA Journal, vol. 37(12), pp 1670-1773, 1999.
[6] A.J. Reynolds, Similarity in Swirling Wakes and Jets, Fluid Mech., vol. 14, pp 241-243, 1962.
[7] G. Birkhoff and E.H. Zarantonello, *Jets, Wakes and Cavities*, Academic Press, New York, 1957.
[8] H. Schlichting, *Boundary Layer Theory*, McGraw-Hill, 1979.
[9] A.I. Serviente and V.C. Patel, Wake of a Self-Propelled Body, Part 1: Momentumless Wake, AIAA Journal, Vol. 38(4), pp 613-619, 2000.
[10] J.P. Comstock (ed.), Principles of Naval Architecture, SNAME, N.Y., 1967.